Drought shifts sorghum root metabolite and microbiome profiles and enriches the stress response factor pipecolic acid

Running title: Bacterial and Metabolite Profiling of Sorghum Roots

Daniel F. Caddell[1,2], Katherine Louie[3,4], Benjamin Bowen[3,4], Julie A. Sievert[5], Joy Hollingsworth[5], Jeffery Dahlberg[5], Elizabeth Purdom[6], Trent Northen[3,4], Devin Coleman-Derr[1,2#]

[1]Plant Gene Expression Center, USDA-ARS, Albany, CA 94710, USA

[2]Plant and Microbial Biology Department, UC Berkeley, Berkeley, CA 94720, USA

[3]Lawrence Berkeley National Laboratory, Berkeley, CA 94720, USA

[4]Joint Genome Institute, Berkeley, CA 94720, USA

[5]Kearney Agricultural Research & Extension Center, Parlier, CA 93648, USA

[6]Department of Statistics, UC Berkeley, Berkeley, CA 94720, USA

[#]Corresponding author: D.Coleman-Derr; E-mail: colemanderr@berkeley.edu

Word count: Abstract- 250 / Main Text- 3,918

Keywords: drought, roots, 16S rRNA, amplicon sequencing, microbiome, metabolomics, pipecolic acid, sorghum

Funding: US Department of Agriculture (CRIS 2030-21430-008-00D), Department of Energy Joint Genome Institute Community Science Program Grant Number: 502952.

ABSTRACT

Interactions between plants and their root-associated microbiome are important for determining host fitness during periods of stress. During drought, monoderm bacteria are more abundant in sorghum roots than in those of watered controls. Additionally, a reversion from monoderm to diderm dominance occurs in drought-stressed roots one week after rewatering. However, the mechanisms driving this rapid microbiome composition shift is currently unknown. To understand if changes in host metabolism are correlated with this shift, we employed 16S amplicon sequencing and metabolomics of root, rhizosphere, and soil at the peak of a preflowering drought and 24 hours after rewatering. The microbiomes of droughted roots, rhizospheres, and soils differed from watered controls, and shifts in bacterial composition were observed in root and rhizosphere 24 hours after rewatering, highlighting the rapid response of microbes to the cessation of drought. Next, we performed metabolomic profiling to identify putative drivers of this process. During drought, we observed a high abundance of abiotic stress response factors, including antioxidants, osmolytes, amino acids, and plant hormones. After rewatering, large shifts in metabolite abundances were observed in rhizosphere, whereas shifts in root and soil were subtle. In addition, pipecolic acid, a well-characterized systemic acquired resistance signalling compound, was enriched in roots and rhizosphere during drought. We found that exogenous application of pipecolic acid suppresses root growth via a systemic acquired resistance-independent mechanism. Collectively, these data provide a comprehensive characterization of metabolite shifts across three compartments during drought, and elucidate a potential role of pipecolic acid in the sorghum drought response.

IMPORTANCE

Plant-associated microbial communities shift in composition and contribute to host fitness during drought. In particular, Actinobacteria are enriched in plant roots and rhizosphere during drought. However, the mechanisms plants use to drive this shift are poorly understood. Here we apply a combination of bacterial and metabolite profiling in root, rhizosphere, and soil during drought and drought-recovery to investigate potential contributions of host metabolism towards shifts in bacterial composition. Our results demonstrate that drought alters metabolic profiles and that the response to rewatering differs between compartments; we identify drought-responsive metabolites that are highly correlated with Actinobacteria abundance. Furthermore, our study reports for the first time that pipecolic acid is a drought-enriched metabolite in sorghum roots. We demonstrate that exogenous application of pipecolic acid is able to provoke one of the classic drought responses in roots, root growth suppression, and that this activity functions independently from the systemic acquired resistance pathway.

INTRODUCTION

Drought is one of the most significant abiotic stresses impacting agricultural production and threatens to become an even bigger concern due to climate change. Root-associated microbial communities, commonly referred to as microbiomes, influence plant responses to a wide-variety of environmental stresses including drought, and are capable of promoting improved fitness (1). In order to engineer microbiomes capable of enhancing plant growth and ameliorating stress, more research is needed to understand

what signals plants use to simultaneously recruit beneficial microbes, while repelling potential pathogens, from a broad pool of soil microbes. Taking advantage of advances in high-throughput sequencing technologies, researchers are beginning to understand the dynamic nature of the microbiome and its association with plant roots. For instance, it is now known that microbiomes vary between environments (2–4), between species (5–7), and even varieties of the same species (4, 8–10). Additionally, microbiomes are dynamic and shift with developmental age, particularly as the plant transitions between vegetative and reproductive growth (11–13). The root microbiome also responds to abiotic stresses. For example, enrichment of monoderm bacteria, such as Actinobacteria, during drought has been observed across diverse plant clades (6, 7, 13, 14). Notably, recent studies have demonstrated that plants mediate the shifts in bacterial communities during drought (15), and Actinobacterial enrichment during drought is dependent on signals produced by living roots (16). While monoderm bacteria are dominant during drought, their enrichment is transitory, with diderm bacteria reestablishing after rewatering (13). Despite their significance, the dynamics regulating monoderm enrichment during drought and the subsequent shift to diderm dominance after rewatering is not yet understood.

Plant-derived metabolites are predicted to drive some of the changes in the root microbiome, as exudation patterns between photoperiods (17) and across development (11, 18, 19) both track with changes in the microbiome. Additionally, a recent study of the maize leaf microbiome across 300 maize genotypes observed associations between specific microbial taxa and host metabolic functions (20). Different combinations of root

93 exudates are sufficient to alter microbiome composition (21), likely by impacting
94 attraction and behavior of soil microbes (22, 23). Some root exudates can act as carbon
95 sources for microbes, while others simultaneously promote certain microbial taxa and
96 suppress others (24). Exudation of putative defense-related metabolites, including
97 organic acids, may also act to repel microbes (23, 25–29). Drought promotes changes
98 in exudate composition, stimulating the exudation of primary and secondary
99 metabolites, including osmoprotectants such as sugars and amino acids. These root
100 and rhizosphere metabolites are predicted to play a role in regulating microbiome
101 associations during drought (30, 31).
102
103 Abiotic stresses also contribute to the modulation of plant immunity through
104 modifications to the balance of many hormone pathways, including abscisic acid (ABA),
105 salicylic acid (SA), jasmonic acid (JA), and ethylene (32). For example, ABA, which is
106 strongly induced by drought, antagonizes systemic acquired resistance (SAR) both
107 upstream and downstream of SA (33). In sorghum (*Sorghum bicolor* (L.) Moench),
108 reduced expression of both SA and JA-responsive genes occurs during a prolonged
109 drought (34). This phenomenon has also been observed in response to other abiotic
110 stresses as well; sorghum has reduced SA biosynthesis during nitrogen-limiting
111 conditions (35), and *Arabidopsis* represses immune signalling genes in response to
112 phosphate stress (36). This modulation has major implications for plant-associated
113 microbiomes, as microbes that colonize plant roots must either evade or suppress host
114 immune responses in order to thrive; mutants deficient in immune activation (37) and
115 exogenous application of plant defense hormones JA (38, 39) and SA (40) are both

116 sufficient to alter root microbiomes. Collectively, these studies support the hypothesis
117 that the plant immune system is in part responsible for regulating the establishment of
118 the root microbiome and is impacted by abiotic stress.
119
120 In this study, we utilize preflowering drought in field grown sorghum to determine if host
121 metabolism drives the enrichment of monoderm bacteria during drought, and whether
122 drought-driven changes in metabolites may play a role in the rapid transition from
123 monoderm to diderm dominance during re-acclimation to watering. Towards this goal,
124 we employed 16S amplicon sequencing and metabolomic profiling of root, rhizosphere,
125 and soil at the peak of drought and 24 hours after rewatering. We observe an
126 enrichment of monoderm bacteria during drought, consistent with previous reports (6, 7,
127 13). Furthermore, we determine that the microbiome responds rapidly to rewatering,
128 particularly in the rhizosphere. We also discover that drought alters the metabolite
129 profiles of sorghum root, rhizosphere, and soil. In particular, known drought-associated
130 metabolites such as betaine, 4-aminobutanoic acid (GABA), and amino acids including
131 proline are enriched during drought. Notably, the abundance of a large number of
132 rhizosphere metabolites are rapidly depleted by rewatering following drought, whereas
133 few metabolites shift abundance in the root. In addition to known drought-associated
134 metabolites, we report the detection of pipecolic acid (Pip), a lysine catabolite that is an
135 essential component of SAR (41, 42), as a drought-enriched metabolite in sorghum.
136 Here, we demonstrate that exogenous application of Pip suppresses plant root growth,
137 and that this activity functions independently from the established SAR pathway.
138

RESULTS

The sorghum root-associated microbiome is influenced by drought and responds rapidly to rewatering

To examine the effect of a prolonged drought on the root microbiome of sorghum, a field experiment was performed at the University of California's Agriculture and Natural (UC-ANR) Resources Kearney Agricultural Research and Extension (KARE) Center, in which sorghum plants were subjected to a prolonged preflowering drought, where no water was applied between planting and the onset of flowering (TP8), or regularly irrigated throughout the experiment (figure 1a). We performed 16S rRNA community profiling of root, rhizosphere, and soil using Illumina MiSeq, targeting the V3-V4 variable regions (figure 1b-j). In agreement with a previous study of the sorghum drought microbiome, which was performed at the same location (13), alpha diversity significantly differed between sample types (Shannon, $F=82.19$, $P=1.36\times10^{-13}$), with lower diversity in the root, as compared with rhizosphere and soil, and reduced diversity in droughted roots compared with watered roots (ANOVA, Tukey-HSD, $P<0.001$) (figure 1c). Beta diversity was assessed through principal coordinates analysis (PCoA) using Bray–Curtis dissimilarities. The primary axis distinguished samples foremost by compartment (root, rhizosphere, or soil), and the second axis by watering regime (droughted or well-watered) (figure 1d), suggesting that both compartment and drought were major driving factors in shaping the microbiome. Pairwise permutational multivariate analysis of variance (PERMANOVA) was performed for each compartment, treatment, and the interaction between compartment and treatment, and all were significantly different ($q<0.05$) (figure 1d).

Similar to previous studies of root microbiomes, we observed a significant enrichment of monoderm bacteria during drought, including taxa belonging to the phylum Actinobacteria in root and rhizosphere, and Firmicutes in the rhizosphere (ANOVA, Tukey-HSD, P<0.05) (figure 1b,e-f). Likewise, diderm lineages were depleted during drought, including Proteobacteria in roots and rhizosphere, Bacteroidetes in roots, and Gemmatimonadetes in the rhizosphere (ANOVA, Tukey-HSD, P<0.05) (figure 1b,g-i). These results suggest that the sorghum root-associated microbiome was responsive to drought, in corroboration with past studies.

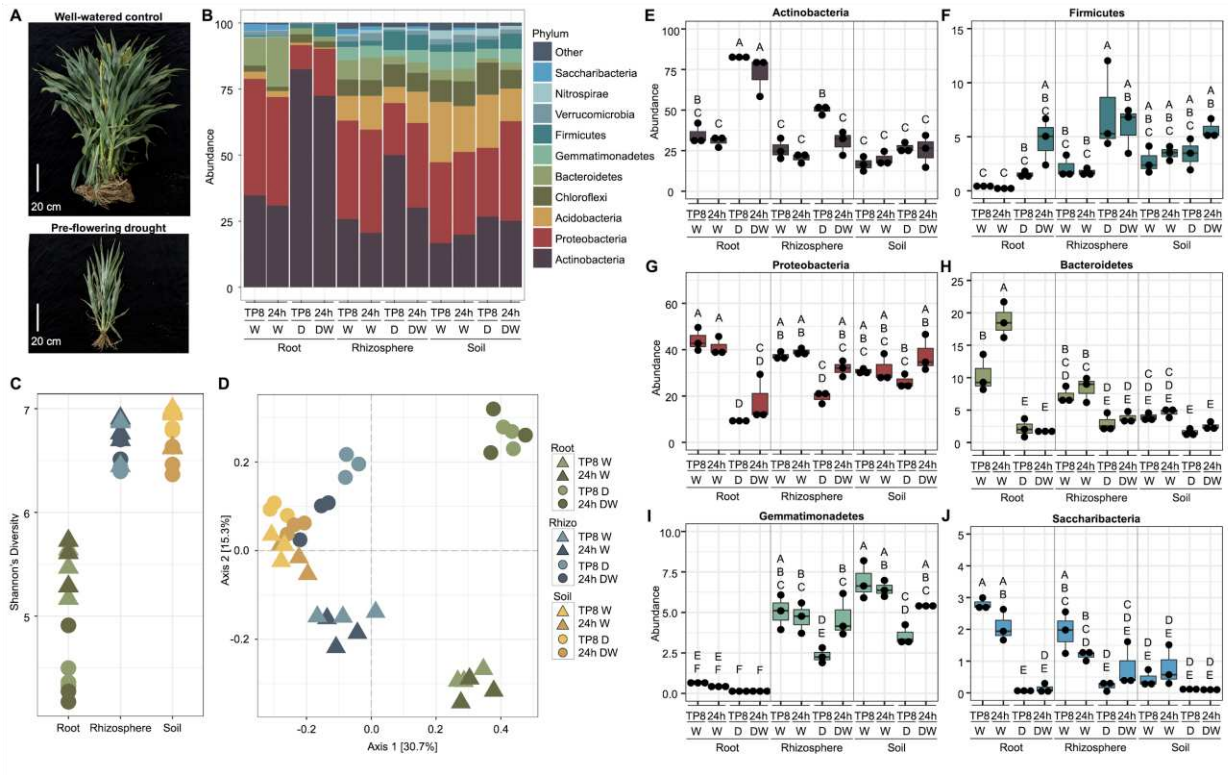

Figure 1. Sorghum root-associated microbiome responds to drought and rewatering. A *Representative image of sorghum plants following eight weeks of a preflowering drought (TP8).* ***B*** *Phylum level relative abundances of sorghum root, rhizosphere, and soil microbiomes at TP8 and 24 hours after rewatering (24h DW) in well-watered (W) or drought (D) plots.* ***C*** *Alpha diversity (Shannon) of sorghum root, rhizosphere, and soil.* ***D*** *Beta diversity (PCoA) of sorghum root, rhizosphere, and soil microbiomes at TP8 and 24 hours after rewatering in well-watered control or drought plots.* ***E-J*** *Relative abundances of individual lineages that displayed a significant difference in abundance between watering treatments* (ANOVA, Tukey-HSD, $P<0.05$).

Following drought, the sorghum root microbiome responds dramatically to rewatering, with a transition from monoderm back to diderm dominance after a one week recovery period (13). To better understand the early dynamics of this response to rewatering, we watered the droughted sorghum plots after sampling at TP8, and another sampling was performed 24 hours later. Notably, no significant shifts in relative abundance of root phyla were observed (figure 1b). However, a depletion in Actinobacteria and an increase in Gemmatimonadetes occurred in the rhizosphere (ANOVA, Tukey-HSD, $P<0.05$) (figure 1b,e,i), consistent with monoderm to diderm transitions previously observed after one week of drought recovery (13). Based on levels of beta diversity, the rewatered rhizosphere microbiome appeared more similar to soil, rather than rhizosphere from control samples (figure 1d). These results suggest that the rhizosphere environment provokes a more rapid return to diderm dominance than the root upon rewatering.

197

198 **Drought alters the metabolite profiles of sorghum root, rhizosphere, and soil**

199 Recently, substrate utilization was determined to drive microbe community assembly in
200 the rhizosphere across developmental age in another member of the grass lineage,
201 *Avena barbata* (19). To determine if differences in metabolic signals contribute to
202 bacterial community assemblage during drought in field grown sorghum, we performed
203 an untargeted liquid chromatography-mass spectrometry based metabolomic profiling of
204 root, rhizosphere, and soil, using the same samples as bacterial profiling described
205 above. Using a metabolite atlas as reference (43), 112 and 122 polar metabolites were
206 predicted in positive and negative ion modes, respectively, which were then combined
207 to give a total of 168 unique metabolites (supplemental figure 1, supplemental tables 1
208 and 2). Within these metabolites, we observed different patterns of enrichment across
209 both compartments and treatments, with individual metabolites that were either drought-
210 enriched or drought-depleted (figure 2a). Principal component analysis (PCA) was
211 performed to understand the relationships between samples. PC1 accounted for 59.5%
212 of the total variation and PC2 accounted for 17.1% of the variation, distinguishing
213 samples by both compartment and watering regime (figure 2b). Next, we aimed to
214 determine metabolites that were significantly enriched *(Log_2 fold change >2, t-test*
215 *p<0.05)* in each compartment during drought. Twenty-eight, 35, and 16 metabolites
216 were significantly enriched during drought in roots, rhizosphere, and soil, respectively
217 (supplemental table 3), with enrichment that was either compartment specific or
218 observed in multiple compartments (figure 2c).

219

Differences in metabolites observed between compartment and watering treatment suggest that these factors may be responsible for driving associations between plants and their root-associated microbiome. We hypothesized that metabolites with large changes in relative abundance, or fold change, between drought and watered treatments may be important for the observed shifts in the microbiome. In droughted roots, we observed increases in the relative abundance of many putative abiotic stress response factors, including amino acids, osmoprotectants, antioxidants, hormones, and organic acids (figure 2d, table 1). Surprisingly, the important drought markers ABA, 1-aminocyclopropane-1-carboxylic acid (1-ACC, the precursor to ethylene), proline and betaine separated into three distinct clusters of enrichment (figure 2d). In contrast, only 3 metabolites were significantly more abundant in watered roots, including xylitol and the phenolics 2,3-dihydroxybenzoic acid and 4-methylcatechol, which are direct catabolism products of salicylic acid and methylsalicylate, respectively (44, 45) (figure 2e, table 1). Collectively, the observed metabolite enrichment patterns are consistent with sorghum roots responding metabolically to drought.

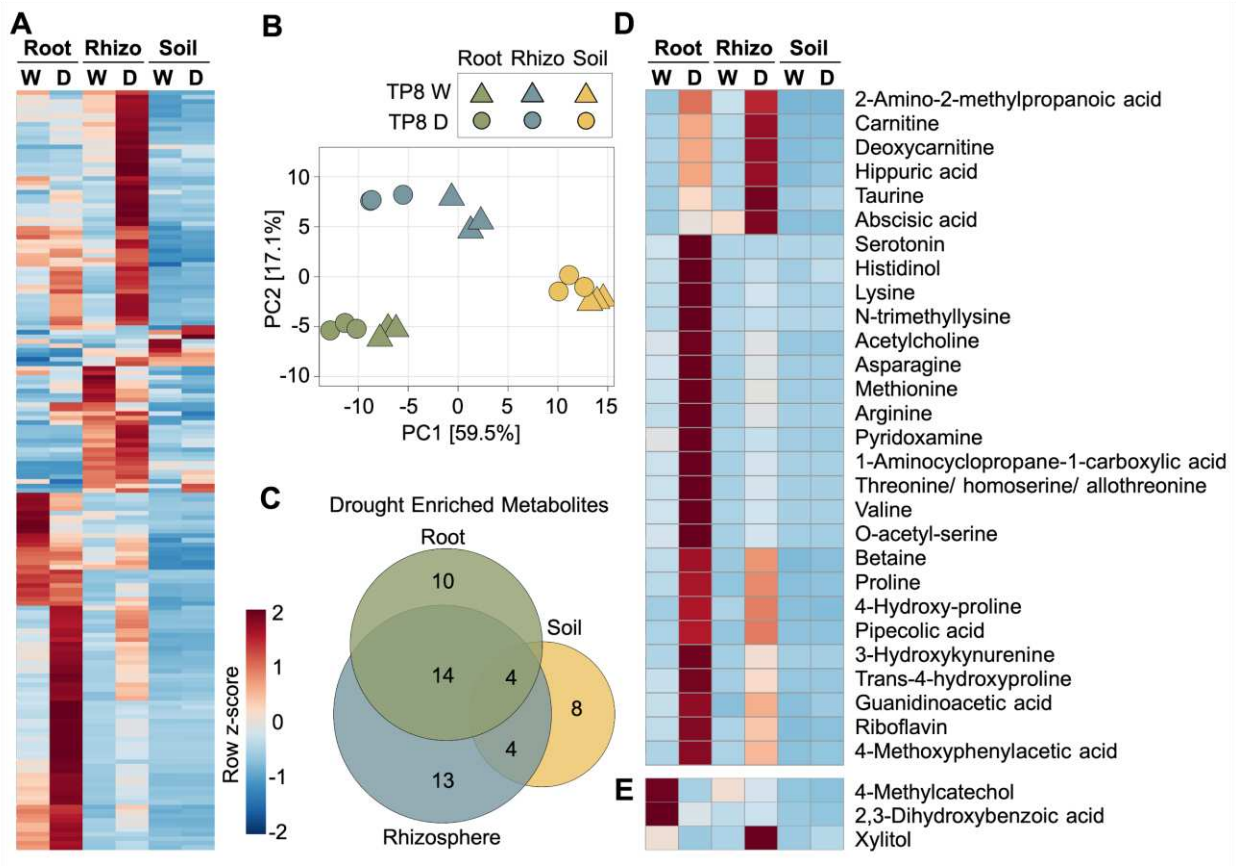

Figure 2. Metabolic profiles during drought differ by compartment. A *Heatmap of relative peak heights of all observed metabolites (n=168) across root, rhizosphere (rhizo), and soil compartments and watered (W) and drought (D) treatments.* ***B*** *Principal component analysis (PCA) plot of root, rhizosphere, and soil metabolites.* ***C*** *Proportional Venn diagram of drought enriched metabolites in root, rhizosphere, or soil (D/W Log_2 fold change >2, t-test p<0.05).* ***D-E*** *Heatmap of the subset of metabolites that were enriched or depleted in roots during drought, with the predicted identity of metabolites listed beside each row.*

Response to rewatering within 24 hours following a prolonged drought varies by compartment

Having established that metabolite composition differs between watered and drought sorghum roots, we next sought to understand whether rapid shifts in metabolite profiles would be observed 24 hours after rewatering the droughted sorghum plots. We hypothesized that rewatering would shift metabolite compositions, particularly in the rhizosphere, that could contribute to the transitions observed in microbial community composition. Consistent with this hypothesis, we observed distinct response patterns in metabolites across all compartments 24 hours after rewatering the droughted plots. Notably, roots were only weakly responsive to rewatering, with no metabolites strongly enriched in rewatered roots (Log_2 fold change >2, t-test $p<0.05$) (figure 3a). However, several metabolites were modestly enriched (Log_2 fold change >1, t-test $p<0.05$), including cytosine, sphinganine, N-acetylglutamic acid, which promotes growth of root hairs and swelling of root tips (46), and ferulic acid, which is capable of inhibiting root growth and promotes root branching (47) (supplemental table 4). Collectively, these shifts suggest roots have started to respond to changes in water availability, although their overall metabolite profiles are largely unchanged at the time of sampling.

In contrast to roots, large shifts in metabolite abundances occurred in the rhizosphere after rewatering, with rewatering tending to cause a depletion of rhizosphere metabolites (figure 3a). Significantly depleted metabolites (n=17, Log_2 fold change < -2, t-test $p<0.05$) included ten different organic acids, four sugar alcohols, sn-glycero-3-phosphocholine, carnitine, and melatonin (figure 3b, table 2). In soil, only a single

metabolite, trehalose, was significantly depleted following rewatering (figure 3c, table 2). Notably, the metabolite composition of rewatered rhizosphere became more similar to watered rhizosphere, and was distinguishable from soil (figure 3d).

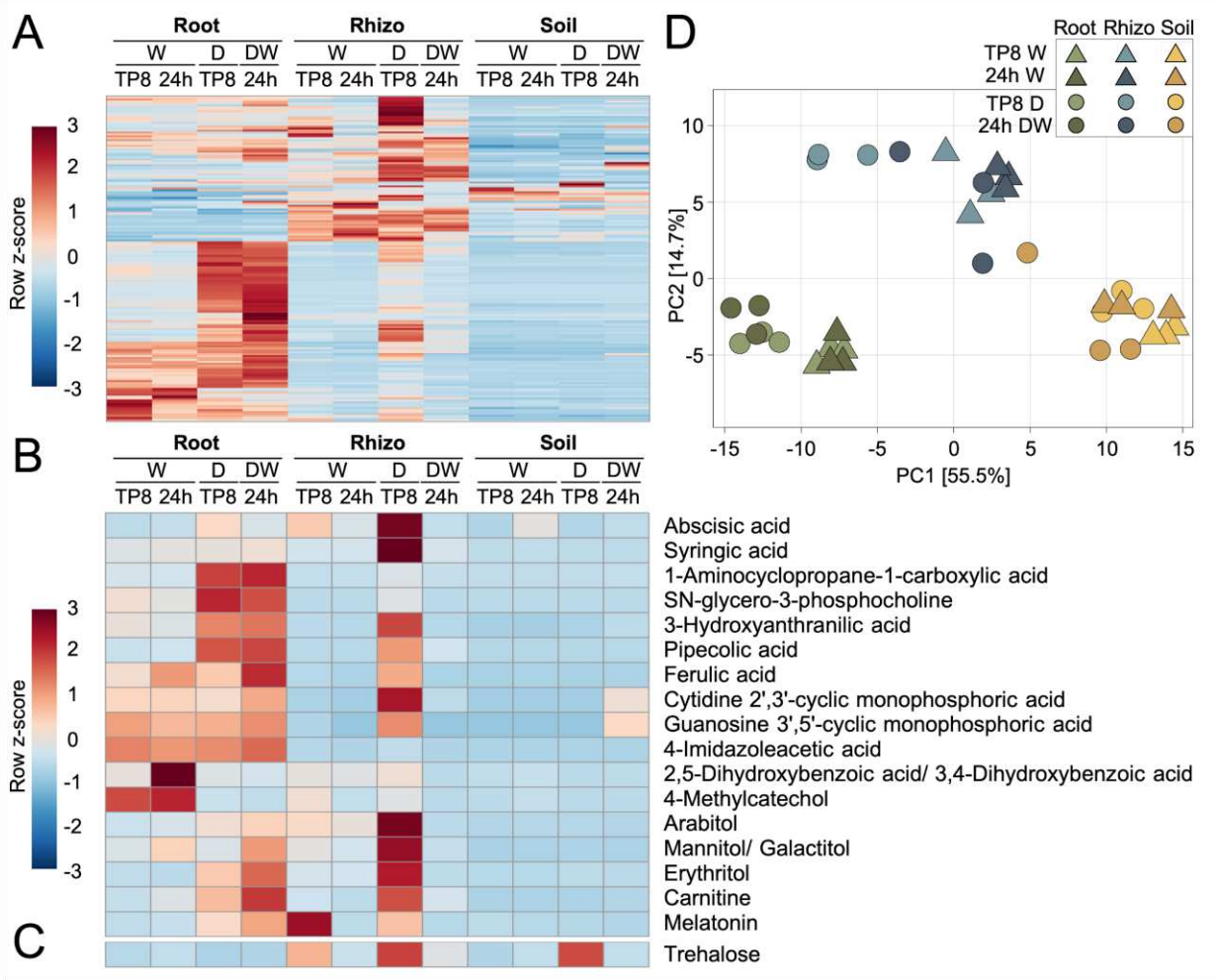

Figure 3. Rewatering depletes rhizosphere metabolites following a prolonged drought. A *Heatmap of relative peak heights of all observed metabolites (n=168) across three compartments (root, rhizosphere (rhizo), and soil), three treatments (watered (W), drought (D), drought rewatered (DW), and two time points (time point 8*

(TP8) and 24 hours later (24h)). ***B-C*** *Heatmap of the subset of metabolites that were depleted after rewatering (DW/D Log_2 fold change < -2, t-test p<0.05), with the predicted identity of metabolites listed beside each row. Note, all significant depletions were observed in the rhizosphere, except trehalose, which occurred in soil.* ***D*** *Principal component analysis (PCA) plot of root, rhizosphere, and soil metabolites.*

Pipecolic acid suppresses plant root growth

Betaine represents one of the most robust and widely utilized biomarkers of plant responses to drought (31, 48). We hypothesized that other metabolites with roles in plant drought response would share a similar abundance pattern during drought. To identify other putative drought metabolites, we ranked metabolites based on their correlation coefficients (Pearson's r) with betaine, across all compartments, treatments, and timepoints (figure 4a-c). The most strongly correlated metabolite, pipecolic acid (Pip), is a lysine catabolite that has recently been identified as a critical component of the systemic acquired resistance (SAR) pathway (41, 42). However, to our knowledge no link between Pip and drought stress response has been demonstrated in plants, although its synthesis is osmotically induced in rapeseed leaf discs (49) and in the halophyte *Triglochin maritima* (50). Beyond Pip, the other nine of the top 10 correlated metabolites have all been previously identified as drought-related metabolites. These include 4-aminobutanoic acid (GABA) (51), allantoin (52, 53), carnitine (54, 55), and the amino acids proline, tyrosine, asparagine, serine, glutamine, and trans-4-hydroxyproline (56–60) (figure 4a).

To identify potential interactions between these drought-related metabolites and the root-associated bacterial community, we clustered bacterial ASVs (grouped at the class level) and metabolites based on abundances across all compartments, treatments, and timepoints. Strikingly, while a majority of metabolites and microbes separated into distinct clusters, three microbial taxa, including the Actinobacteria, nested within the metabolite-dominant cluster, just adjacent to the metabolite cluster containing the top ten betaine-correlated metabolites (supplemental figure 2). When clustering was performed based on the abundances in the root, where host control of the microbiome is strongest, we observed that the Actinobacteria formed an even closer linkage with betaine-correlated metabolites, and was tightly clustered with five metabolites including trans-4-hydroxyproline, proline, Pip, valine, and guanidinoacetic acid (figure 4e-f, supplemental figure 3). As previous reports have demonstrated that drought-induced microbial lineages including Actinobacteria in roots are capable of inducing SAR (61) and systemic root-to-root signaling (62), we hypothesized that the increased abundance of Actinobacteria in sorghum roots may contribute to the accumulation of Pip during drought, and potentially the activation of systemic signaling. However, azelaic acid, which functions downstream of Pip in the SAR pathway (63), was not enriched by drought in our data, suggesting that SAR was not being activated (figure 4d). Collectively, these results suggest that Pip may play an as-yet undiscovered role in sorghum drought response.

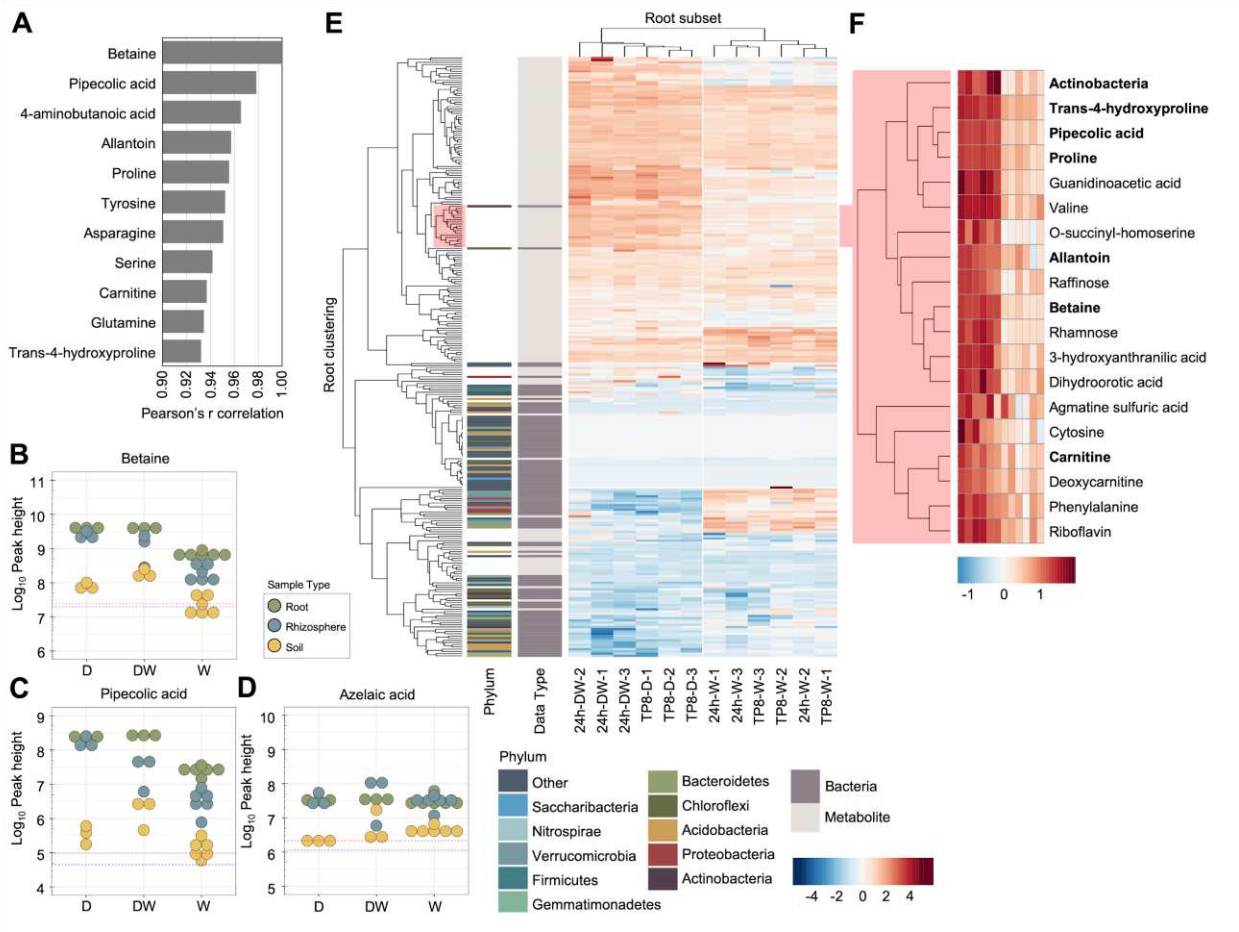

Figure 4. Pipecolic acid abundance pattern mirrors drought markers. A *The top 10 metabolites correlated with the drought marker betaine across all sample types, treatments, and time points.* ***B-D*** *Log_{10} peak heights of individual metabolites. Each point represents an individual sample of root (green), rhizosphere (blue), or soil (yellow). Dashed lines represent the limit of detection for individual metabolites, based on the average log_{10} peak heights of the sample blanks for root (red) or rhizosphere and soil (blue).* ***E*** *Heatmap of relative abundance of all metabolites and bacteria ASVs (grouped at the class level), clustered within the root, across treatments (watered (W), drought (D), drought rewatered (DW), and time points (time point 8 (TP8) and 24 hours later*

(24h)). ***F*** *Zoom-in of Actinobacteria and closely clustering root metabolites, as highlighted in pink in figure 4e. Actinobacteria and the metabolites that are closely correlated with betaine (as in figure 4a) are in bold.*

One classic and easily observable phenotypic shift that occurs in roots during drought is a suppression of root growth (64, 65). We hypothesized that if Pip plays an integral role in the drought response pathway, application of Pip should lead to reduced root growth. To evaluate this possibility, we germinated sorghum in petri dishes containing water plus 0, 0.1, or 1 mM Pip. Seven days after germination, 1 mM Pip treated sorghum displayed significantly reduced root growth (figure 5a-b). Exogenous Pip application is also capable of reducing root growth in *Arabidopsis* (66). We confirmed this result by growing *Arabidopsis* Col-0 on petri dishes containing either 0, 0.001, 0.01, 0.1, 1 mM Pip. Average root growth was reduced in all Pip treatments in a dosage dependent manner, with significant decreases in root growth observed with 0.1 and 1 mM Pip concentrations (figure 5c-d).

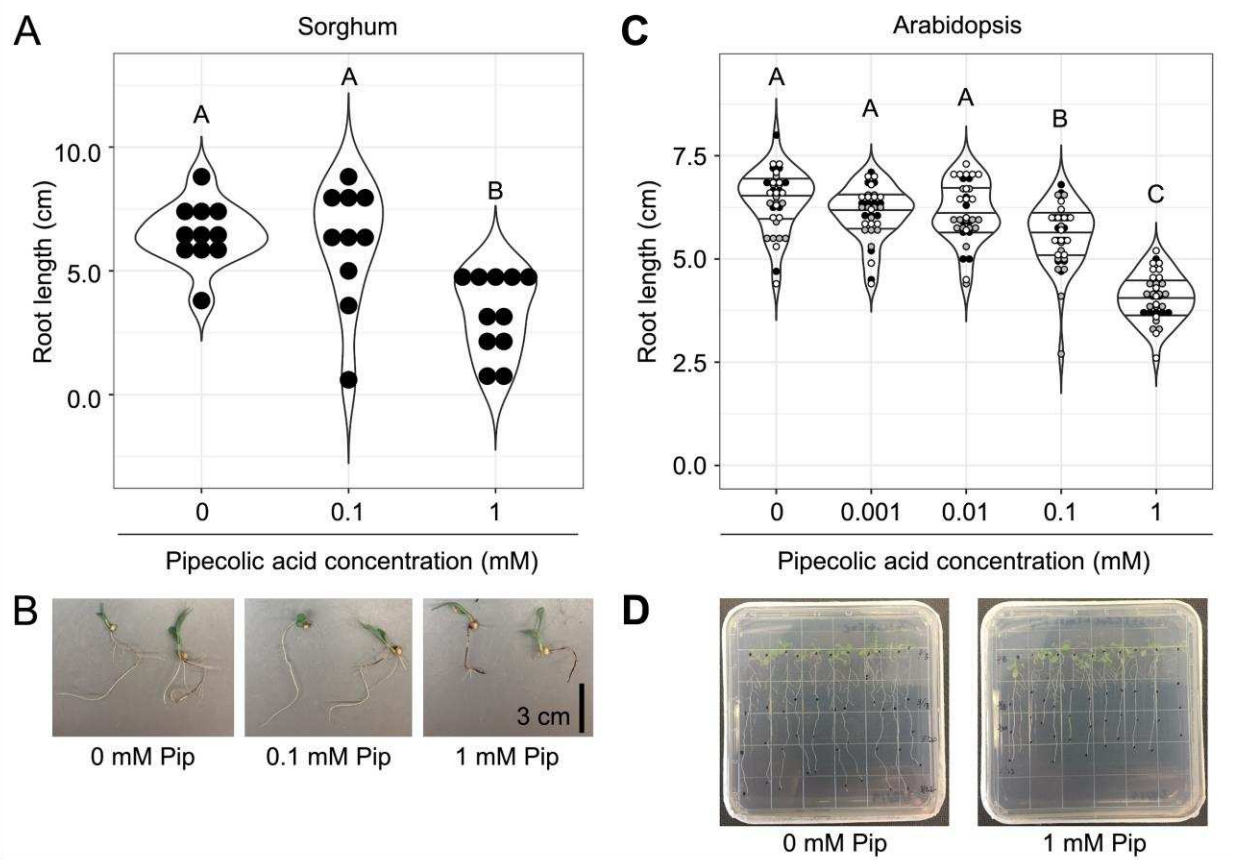

Figure 5. Pipecolic acid reduces root growth. A *Root lengths of sterilized sorghum seedlings after 7 days of growth in water containing 0, 0.1, or 1 mM pipecolic acid (Pip). Different letters indicate a significant difference in root length (ANOVA, Tukey-HSD, p<0.05). This experiment was performed twice with similar results.* ***B*** *Two representative seedlings from each treatment were photographed at the time of measurement.* ***C*** *Root lengths of sterilized Arabidopsis seedlings after 10 days of growth in ½ MS+ 1% sucrose agar media containing 0, 0.001, 0.01, 0.1, or 1 mM Pip. Different letters indicate a significant difference in root length (ANOVA, Tukey-HSD, p<0.05). Different colors represent plants from independent experiments (n=3).* ***D*** *One*

362 *representative plate from 0 and 1 mM pipecolic acid treatments were photographed at*
363 *the time of measurement.*
364
365 Having confirmed that exogenous Pip is sufficient to reduce root growth, we next aimed
366 to understand the molecular mechanism responsible for this behavior. As Pip plays a
367 key role in systemic signalling during SAR (67), we hypothesized that Pip-mediated root
368 growth reduction may depend on components of this signalling pathway. To test this
369 hypothesis, we utilized publicly available genetic resources in *Arabidopsis*, including
370 *fmo-1*, *npr1-1*, *rbohd/rbohf*, *azi1-2* mutants, which represent critical aspects of the SAR
371 signalling pathway (figure 6). We measured the root growth of each of these validated
372 *Arabidopsis* SAR mutants on media containing 1 mM Pip. Notably, mutants in FLAVIN-
373 CONTAINING MONOOXYGENASE 1 (FMO-1), responsible for conversion of Pip to N-
374 hydroxy-Pip (68)(figure 6), displayed reduced root growth similar to the wild-type plant
375 Col-0 in response to Pip (figure 6), indicating that this conversion is not required to elicit
376 reduced root growth. Likewise, mutants in NON EXPRESSER OF PATHOGENESIS
377 RELATED GENES 1 (NPR1) (69), a SA receptor required for SA-dependent SAR, and
378 mutants in NADPH/RESPIRATORY BURST OXIDASE PROTEINS D and F (RBOH
379 D/F) and the lipid transfer protein AZELAIC ACID INDUCED 1 (AZI1) (70, 71), required
380 for SA-independent SAR, also responded similar to Col-0 (figure 6).Collectively, these
381 data indicate that root growth response to Pip is likely not mediated by the SAR
382 pathway.
383

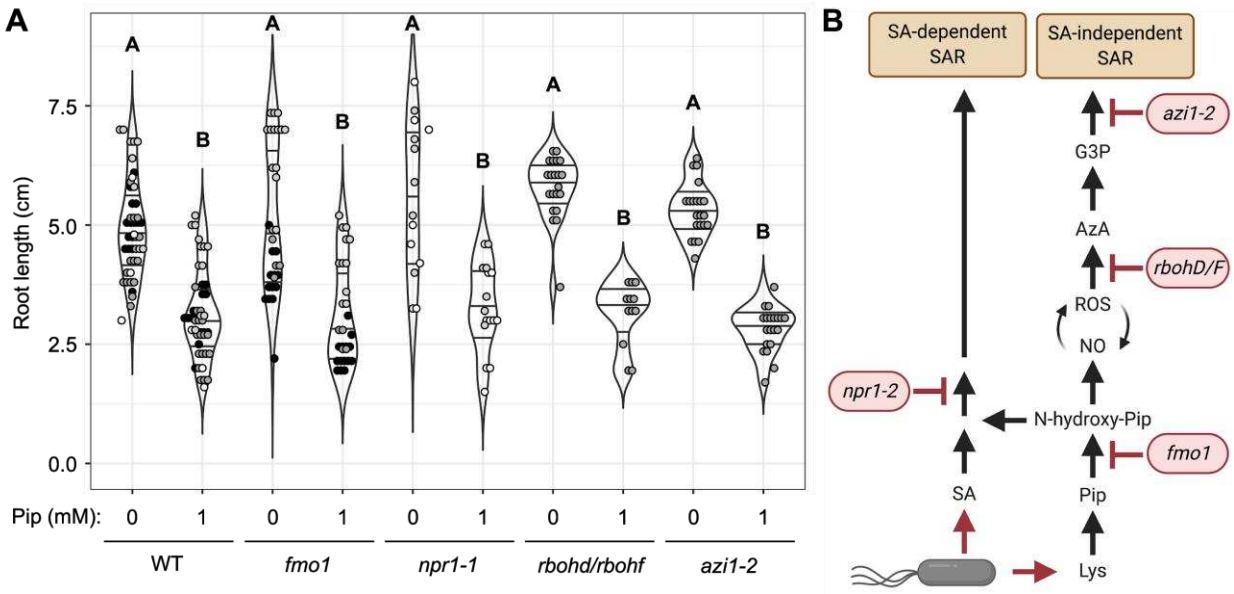

Figure 6. Pipecolic acid root growth reduction is SAR-independent. A *Root length of Arabidopsis Col-0 (WT) and Arabidopsis mutants grown on 1/2MS + 1% sucrose plates containing 0 or 1 mM Pip. Significance between treatments was evaluated by ANOVA with Tukey's HSD posthoc test ($p<0.05$). Different colors represent plants from independent experiments.* ***B*** *Simplified SAR pathway. Highlighted in red are the Arabidopsis mutants used to evaluate a potential interaction between SAR and Pip-mediated root growth suppression.*

DISCUSSION

Metabolite and microbial community compositions shift during drought and rewatering

The assemblage of the microbiomes differ between root, rhizosphere, and soil during drought, though the underlying cause of these differences is not well understood. Plant metabolites and exudates have been hypothesized to drive these changes (30), and

plants are known to increase total organic carbon and root exudation (per gram of root biomass) in response to drought (72, 73). The enrichment of specific metabolites that can act as osmoprotectants, such as betaine, sugars, and amino acids, is frequently reported when plants are subjected to drought, and these are commonly used as drought-specific markers. Yet, comprehensive studies of the global metabolite profiles across root, rhizosphere, and soil have been hindered by the complexity of soil metabolite profiles. However, recent advances in metabolomics have allowed for characterization of metabolite profiles within and across complex substrates (74). As a result, we collected both microbiome and metabolite profiles across three different compartments (sorghum root, rhizosphere, and soil) and three treatments (watered, drought, and drought recovery). We observed a general trend that many metabolites were more abundant during drought. This observation is in line with previous evidence that exudation by plants increases during drought (72). Interestingly, we observed both shifts in metabolite abundances during drought that were compartment specific and shifts that occurred across multiple compartments. Likewise, we observed enrichment of specific drought responsive metabolites that correlated with increases in both monoderm dominance during drought and compartment specific shifts upon rewatering. Our findings that changes in host metabolism during drought are correlated with shifts in certain bacterial taxa expand upon a recent finding that substrate utilization also drives microbial community assembly in the rhizosphere across developmental age (19).

A previous study of sorghum root and rhizosphere showed that bacterial community abundance reverts from monoderm dominance during drought to diderm dominance

423 within a week following rewatering (13). To understand the early dynamics of this
424 reversion, we evaluated sorghum root, rhizosphere, and soil at the peak of a
425 preflowering drought and again 24 hours after rewatering. We observed distinct
426 response patterns in metabolites of root, rhizosphere, and soil 24 hours after
427 rewatering, which could impact the establishment of microbiomes following rewatering.
428 Notably, the rhizosphere was the most responsive in both metabolites and microbiome
429 profiles within 24 hours after rewatering. We propose that the more rapid shifts
430 observed in rhizosphere are largely driven by flow of water, which may simultaneously
431 dilute rhizosphere metabolites into the surrounding soil, and promote the mobility of soil
432 microbes to enter the rhizosphere. Supporting this hypothesis, the beta diversity of
433 rewatered rhizosphere microbiome early after rewatering more closely resembled the
434 soil microbiome, rather than watered rhizosphere samples, suggesting that the soil
435 microbiome is a source of inoculum for bacterial establishment in the rhizosphere
436 following rewatering. In contrast, rhizosphere metabolites were characterized by
437 depletion after rewatering, with similarity to watered rhizosphere, which may facilitate
438 the eventual reversion to a watered rhizosphere microbiome, as demonstrated
439 previously (13). Comparable studies on the long-term effects of drought and subsequent
440 rewatering on metabolite profiles in grasses are lacking, however previous studies of
441 trees have reported mixed long-term effects. One study found that increases in
442 exudation can be reversed following recovery from drought, to be indistinguishable from
443 controls (73), while another found that extreme drought led to irreversible changes in
444 exudation (59). Therefore, future studies will benefit from careful selection of multiple

time points following drought to understand the long-term effects of drought in roots and rhizosphere following rewatering.

Pipecolic acid-mediated root growth suppression is not mediated by the systemic acquired resistance pathway

In this study, we observed an enrichment of many putative abiotic stress response factors during drought. Of particular note, Pip was significantly enriched during drought, and its abundance correlated strongly with other highly enriched drought markers including Actinobacteria and the metabolites betaine, proline, and GABA. While Pip induction in response to osmotic stress has been noted in a few previous studies (49, 50), by far Pip's most notable role is in systemic signalling of stress in response to pathogens. It has recently been shown that the conversion of Pip to N-hydroxy-Pip is required for SAR to be activated, and this activity functions both alongside and independent of SA (67, 75). Notably, previous research has demonstrated that "biotic stress" factors, including SA, can benefit plants responding to abiotic stress. For example, plant drought tolerance can be promoted by increasing endogenous SA in *Arabidopsis* (76), and exogenous SA also promoted drought tolerance via an NPR1-dependent mechanism in *Brassica napus* (77). However, recent studies suggest that SA signaling is inactivated by drought, in part because ABA promotes NPR1 degradation (33, 78). Additionally, a strong suppression of defense-related gene expression occurs in field grown sorghum during preflowering drought (34). Likewise, we did not see an enrichment of azelaic acid, which functions downstream of Pip during SAR, during drought in our data. These findings suggest that the Pip induction observed during

468 drought is likely acting for some other purpose, perhaps as an independent signalling
469 mechanism related to abiotic stress.
470
471 Here, we demonstrate that Pip application is able to provoke one of the classic drought
472 responses in roots, namely root growth suppression (64, 65), which suggests it could be
473 involved in the drought response pathway. As exogenous Pip was capable of
474 suppressing root growth in both sorghum and *Arabidopsis*, this suggests that a common
475 mechanism is conserved across plants. We hypothesized that Pip-mediated root growth
476 suppression might share components with the SAR pathway, which functions across
477 diverse plant clades (79). However, using previously validated *Arabidopsis* SAR
478 pathway mutants, we demonstrate that this Pip activity in the root functions
479 independently from the established SAR pathway, which has primarily been evaluated
480 in leaves. These data suggest that although Pip has been primarily characterized as a
481 component of SAR in plants, it may also act as a more general stress response factor to
482 environmental shifts including drought using an alternative mechanism. Furthermore,
483 azelaic acid, another component of SAR that functions downstream of Pip, is not
484 enriched in sorghum roots under drought, which suggests that this pathway, if it exists,
485 acts differently than the one currently known example.
486
487 Interestingly, Pip, which was significantly enriched in both roots and rhizosphere, has
488 also been shown to have a direct role on microbes, where it is predicted to function in
489 osmoprotection. For example, Pip has been widely demonstrated to improve the growth
490 of a diverse bacteria challenged by NaCl-induced osmotic stress, including the

Actinobacteria lineage *Brevibacterium ammonkgenes* (80), and Proteobacteria lineages *Escherichia coli* (81), *Sinorhizobium meliloti* (82), and *Silicibacter pomeroyi* (83). Supporting its role as an osmoprotectant, exogenous application of another osmoprotectant, betaine, suppressed the salt-induced accumulation of Pip (80). These studies support a possible role of rhizosphere Pip acting as an osmolyte to protect bacteria during drought. However, as Pip appears to be functional across a broad range of bacterial lineages, we do not believe Pip is likely to be responsible for the shifts in monoderm and diderm dominance observed during drought and subsequent rewatering. Collectively, our results highlight the need for future studies that delve further into the potential contribution(s) of Pip to plant drought responses.

METHODS

Field experimental design and sample collection

Sorghum cultivar RTx430 plants were grown in the summer of 2017, in a field located at the UC-ANR KARE Center located in Parlier, California (36.6008 N 119.5109 W), as described previously (13, 84). Sorghum seeds were sown into pre-watered fields. Starting in the third week, control treatment plants were watered 1h three times per week by drip irrigation (1.89 L h− 1 flow rate), and no water was provided to drought treatment plants. After eight weeks, which coincided with the onset of flowering, roots and rhizosphere samples were harvested prior to watering (TP8). Water was then restored to the drought plots (rewatered), and root and rhizosphere samples were harvested after 24 h (TP8+24h). All field samples were collected between 11am and 12pm using a modified version of the protocol described in detail in (85). Soil samples

514 were collected using a 15 cm soil core sampler, at a distance of approximately 20 cm
515 from the base of the plant. To collect rhizosphere compatible with both microbiome and
516 metabolomic analyses, excavated plants were briefly shaken to dislodge excess soil,
517 and an ethanol-sterilized nylon bristled toothbrush was used to remove closely adhering
518 soil from the root, which we collected as the rhizosphere fraction, prior to vortexing the
519 roots two times for 1 min in epiphyte removal buffer (ice cold 0.75% KH_2PO_4, 0.95%
520 K_2HPO_4, 1% Triton X-100 in ddH_2O; filter sterilized at 0.2 µM). Any remaining soil
521 adhering to the root was separated with epiphyte removal buffer and discarded. The
522 roots were again rinsed with clean epiphyte removal buffer and patted dry. All samples
523 were immediately flash frozen in LN_2 in the field and stored at -80 °C until sample
524 processing.
525
526 **DNA extraction, amplification, and amplicon sequencing**
527 DNA extraction was performed using the protocol for collection of root endosphere,
528 rhizosphere, and soil samples using Qiagen DNeasy Powersoil DNA extraction Kit with
529 0.15 g (root) and 0.25 g (rhizosphere and soil) as starting material in the provided
530 Powersoil collection vials, as described in detail in (85). The V3-V4 region of the 16S
531 rRNA gene was PCR amplified from 25 ng of genomic DNA using dual-indexed 16S
532 rRNA Illumina iTags 341F (5'-CCTACGGGNBGCASCAG-3') and 785R (5'-
533 GACTACNVGGGTATCTAATCC-3'). Barcoded 16S rRNA amplicons were quantified
534 using Qubit dsDNA HS assay kit on a Qubit 3.0 fluorometer (Invitrogen, Carlsbad, CA,
535 USA), pooled in equimolar concentrations, purified using Agencourt AMPure XP
536 magnetic beads (Beckman Coulter, Indianapolis, IN, USA), quantified using Qubit

dsDNA HS assay kit on a Qubit 3.0 fluorometer (Invitrogen, Carlsbad, CA, USA), and diluted to 10 nM in 30 µL total volume before submitting to the QB3 Vincent J. Coates Genomics Sequencing Laboratory facility at the University of California, Berkeley for sequencing using Illumina Miseq 300 bp pair-end with v3 chemistry.

Amplicon sequence processing and analysis

16S amplicon sequencing reads were demultiplexed in QIIME2 (86) and then passed to DADA2 (87) to generate Amplicon Sequence Variants (ASVs), with taxonomies assigned using the August 2013 version of GreenGenes 16S rRNA gene database as described previously (16). All subsequent 16S statistical analyses were performed in R-v3.6.1 (88). To account for differences in sequencing read depth across samples, samples were normalized by dividing the reads per ASV in a sample by the sum of usable reads in that sample, resulting in a table of relative abundance frequencies, which were used for analyses, with the exception of alpha-diversity calculations, for which all samples were normalized to an even read depth of 29,918 ASVs per sample. Alpha diversity was determined with the estimate_richness function in the R package phyloseq-v1.30.0 (89), and significance was tested by ANOVA using the aov function in the R stats package. Beta diversity (PCoA) was performed using the ordinate function in the R package phyloseq-v1.30.0 (89). Sample type separation was determined by pairwise PERMANOVA with 1,000 permutations using the adonis and calc_pairwise_permanovas functions in the R packages vegan-v2.5.6 (90) and mctoolsr-v0.1.1.2. Tukey-HSD tests used the HSD.test function in the R package

559 Agricolae-v1.3.1. The combined metabolite and bacterial ASV heatmaps were
560 generated using the R package pheatmap-v1.0.12.
561
562 **Metabolite extraction and LC-MS**
563 Root water content was estimated by lyophilizing root tissue and calculating the
564 difference between wet and dry weights. Root samples for submission were then
565 normalized such that the lightest sample was 0.2 g (wet weight) and each other sample
566 was at least 0.2 g. Rhizosphere and soil water contents were estimated to obtain similar
567 amounts of material. The overall difference in percent water content between samples
568 was minimal (2.5-6.5%). For extraction of polar metabolites from root tissue (0.2-0.3 g
569 wet weight), samples were first lyophilized dry, then 500 µL of methanol was added,
570 followed by a brief vortex and sonication in a water bath for 10 min. Samples were
571 centrifuged 5 min at 5,000 rpm, then supernatant transferred to 2 mL tubes, dried in a
572 SpeedVac (SPD111V, Thermo Scientific, Waltham, MA), and extracts stored at -80 °C.
573 For soil and rhizosphere samples (1.25 g wet weight), polar metabolites were extracted
574 similarly but samples were not lyophilized prior to extraction, 2 mL LC-MS grade water
575 was added followed by vortex and water bath sonication for 30 min, centrifugation for 7
576 min at 7,000 rpm, then supernatant transferred to a 5 mL tube, frozen and lyophilized
577 dry, and extracts stored at -80 °C.
578
579 In preparation for LC-MS, soil and rhizosphere extracts were resuspended with 300 µL
580 methanol containing internal standards (~15 µM average of 5-50 µM of 13C,15N Cell
581 Free Amino Acid Mixture; 4-(3,3-dimethyl-ureido)benzoic acid; 3,6-dihydroxy-4-

582 methylbenzoic acid; d5-benzoic acid; 9-anthracene carboxylic acid; 13C-trehalose; 13C-
583 mannitol), vortexed and sonicated 10 min, centrifuged 5 min at 5,000 rpm, supernatant
584 centrifuge-filtered 2.5 min at 2 500 rpm (0.22 µm hydrophilic PVDF), then 150 µL
585 transferred to LC-MS glass autosampler vials. Root extracts were resuspended
586 similarly, but with resuspension volume varied to normalize by root dry weight.
587
588 Chromatography was performed using an Agilent 1,290 LC stack, with MS and MS/MS
589 data collected using a Thermo QExactive Orbitrap MS (Thermo Scientific, Waltham,
590 MA). Full MS spectra were collected from *m/z* 70-1,050 at 70,000 resolution in both
591 positive and negative ion modes, with MS/MS fragmentation data acquired using
592 stepped 10, 20, and 40 eV collision energies at 17,500 resolution. Chromatography was
593 performed using a HILIC column (Agilent InfinityLab Poroshell 120 HILIC-Z, 2.1 x 150
594 mm, 2.7 µm, #673775-924) at a flow rate of 0.45 mL/min with a 2 µL injection volume.
595 To detect metabolites, samples were run on the HILIC column at 40 ºC equilibrated with
596 100% buffer B (95:5 ACN:H2O with 5 mM ammonium acetate) for 1 min, diluting buffer
597 B down to 89% with buffer A (100% H2O with 5 mM ammonium acetate and 5 µM
598 methylenediphosphonic acid) over 10 min, down to 70% B over 4.75 min, then down to
599 20% B over 0.5 min, followed by isocratic elution in 80% buffer A for 2.25 min. Samples
600 consisted of 3 biological replicates each and 3 extraction controls, with sample injection
601 order randomized and an injection blank (2 µL MeOH) run between each sample.
602
603 **Metabolite identification and analysis**

Metabolite identification was based on exact mass and comparing retention time (RT) and MS/MS fragmentation spectra to that of standards run using the same chromatography and MS/MS method. Custom Python code (91) was used to analyze LC-MS data. For each feature detected (unique *m/z* coupled with RT), a score (0 to 3) was assigned representing the level of confidence in the metabolite identification. Positive identification of a metabolite had detected m/z ≤ 5 ppm or 0.001 Da from theoretical as well as RT ≤ 0.5 min compared to a pure standard run using the same LC-MS method. The highest level of positive identification (score of 3) for a metabolite also had matching MS/MS fragmentation spectra compared to either an outside database (METLIN) (92) or internal database generated from standards run and collected on a QExactive Orbitrap MS. Identifications were invalidated if MS/MS from the sample mismatched that of the standard. MS/MS mirror plots for metabolites are presented in supplemental figure 1.

A total of 112 and 122 polar metabolites were predicted in positive and negative ion modes respectively (supplemental table 1). If a metabolite was observed in both ion modes, the mode with higher peak height was selected for the merged metabolite profile (n=168) used for all analyses. Values below the limit of detection were imputed with the lowest observed values in the dataset rounded down (2,400 or 1,900 for positive or negative ion modes respectively) (supplemental table 2). Principal components analysis of metabolite profiles was performed using the prcomp function in the R stats package. Venn diagram construction utilized Venny-v2.1.0 (93). All other metabolite analyses were performed using MetaboAnalyst-v4.0 (94, 95). Heatmaps

were generated using Euclidean distance and Ward clustering algorithms. We evaluated enriched or depleted metabolites with the cutoffs of $\log_2$ fold change greater than 2 or less than -2, and a p-value of less than 0.05.

Plant root growth assays

Sterilized seeds of the sorghum cultivar RTx430 were germinated on petri dishes with autoclaved Milli-Q water or autoclaved Milli-Q water containing the defined concentration of Pip overnight in the dark at 28 °C, before being transferred to a growth chamber (28/22 °C, 16 h day, ppf ~250 µmol $m^{-2}s^{-1}$). The *Arabidopsis* ecotype Columbia (Col-0) was used in this study. Mutant lines *fmo-1* (SALK_026163) (96), *npr1-1* (CS3726) (97), *rbohd/rbohf* (CS68522) (98), and *azi1-2* (SALK_085727) (70) were obtained from the Arabidopsis Biological Resource Center (99). Sterilized seeds were grown on MS plates containing 1/2× Murashige and Skoog salt mix, 1% sucrose (pH 5.8), 0.8% agar, and the defined concentration of Pip. Plants were first stratified for 3 days at 4°C before being transferred to a growth chamber (21 °C, 16 h day, ppf ~120 µmol $m^{-2}s^{-1}$). Root lengths were measured using ImageJ-v1.52a software (100). ANOVA was performed using the aov function in the R stats package and Tukey-HSD tests used the HSD.test function in the R package Agricolae-v1.3.1. SAR pathway image in figure 6b was created with BioRender.com.

Data availability

All datasets and scripts for analysis are available through github (https://github.com/colemanderr-lab/Caddell-2020) and all short read data can be

accessed through NCBI BioProject PRJNA655744. Raw metabolomics data will be made available through the Joint Genome Institute Genome Portal.

Acknowledgements

We thank Dr. Edi Wipf for their helpful discussions and critical reading of the manuscript.

Author contributions

D.C. conceived and designed the experiments, performed the experiments, analyzed the data, and prepared figures and/or tables; K.L.,B.B., and T.N. performed the LC-MS, metabolite identification, and analyzed the data; E.P. analyzed the data and prepared figures and/or tables; J.S., J.H., and J.D. performed the field experiment; D.C-D. conceived and designed the experiments and analyzed the data; All authors authored or reviewed drafts of the paper and approved the final draft.

References cited

1. Zolla G, Badri DV, Bakker MG, Manter DK, Vivanco JM. 2013. Soil microbiomes vary in their ability to confer drought tolerance to Arabidopsis. Appl Soil Ecol 68:1–9.

2. Bulgarelli D, Rott M, Schlaeppi K, Ver Loren van Themaat E, Ahmadinejad N, Assenza F, Rauf P, Huettel B, Reinhardt R, Schmelzer E, Peplies J, Gloeckner FO, Amann R, Eickhorst T, Schulze-Lefert P. 2012. Revealing structure and assembly cues for Arabidopsis root-inhabiting bacterial microbiota. Nature 488:91–95.

673 3. Lundberg DS, Lebeis SL, Paredes SH, Yourstone S, Gehring J, Malfatti S,
674 Tremblay J, Engelbrektson A, Kunin V, Del Rio TG, Edgar RC, Eickhorst T, Ley RE,
675 Hugenholtz P, Tringe SG, Dangl JL. 2012. Defining the core Arabidopsis thaliana
676 root microbiome. Nature 488:86–90.

677 4. Peiffer JA, Spor A, Koren O, Jin Z, Tringe SG, Dangl JL, Buckler ES, Ley RE. 2013.
678 Diversity and heritability of the maize rhizosphere microbiome under field
679 conditions. Proc Natl Acad Sci U S A 110:6548–6553.

680 5. Ofek-Lalzar M, Sela N, Goldman-Voronov M, Green SJ, Hadar Y, Minz D. 2014.
681 Niche and host-associated functional signatures of the root surface microbiome. Nat
682 Commun 5:4950.

683 6. Naylor D, DeGraaf S, Purdom E, Coleman-Derr D. 2017. Drought and host
684 selection influence bacterial community dynamics in the grass root microbiome.
685 ISME J.

686 7. Fitzpatrick CR, Copeland J, Wang PW, Guttman DS, Kotanen PM, Johnson MTJ.
687 2018. Assembly and ecological function of the root microbiome across angiosperm
688 plant species. Proc Natl Acad Sci U S A 115:E1157–E1165.

689 8. Edwards J, Johnson C, Santos-Medellín C, Lurie E, Podishetty NK, Bhatnagar S,
690 Eisen JA, Sundaresan V. 2015. Structure, variation, and assembly of the root-
691 associated microbiomes of rice. Proc Natl Acad Sci U S A 112:E911–20.

692 9. Haney CH, Samuel BS, Bush J, Ausubel FM. 2015. Associations with rhizosphere
693 bacteria can confer an adaptive advantage to plants. Nat Plants 1.

10. Walitang DI, Kim C-G, Kim K, Kang Y, Kim YK, Sa T. 2018. The influence of host genotype and salt stress on the seed endophytic community of salt-sensitive and salt-tolerant rice cultivars. BMC Plant Biol 18:51.

11. Chaparro JM, Badri DV, Vivanco JM. 2014. Rhizosphere microbiome assemblage is affected by plant development. ISME J 8:790–803.

12. Edwards JA, Santos-Medellín CM, Liechty ZS, Nguyen B, Lurie E, Eason S, Phillips G, Sundaresan V. 2018. Compositional shifts in root-associated bacterial and archaeal microbiota track the plant life cycle in field-grown rice. PLoS Biol 16:e2003862.

13. Xu L, Naylor D, Dong Z, Simmons T, Pierroz G, Hixson KK, Kim Y-M, Zink EM, Engbrecht KM, Wang Y, Gao C, DeGraaf S, Madera MA, Sievert JA, Hollingsworth J, Birdseye D, Scheller HV, Hutmacher R, Dahlberg J, Jansson C, Taylor JW, Lemaux PG, Coleman-Derr D. 2018. Drought delays development of the sorghum root microbiome and enriches for monoderm bacteria. Proc Natl Acad Sci U S A 201717308.

14. Santos-Medellín C, Edwards J, Liechty Z, Nguyen B, Sundaresan V. 2017. Drought Stress Results in a Compartment-Specific Restructuring of the Rice Root-Associated Microbiomes. MBio 8.

15. Koyama A, Steinweg JM, Haddix ML, Dukes JS, Wallenstein MD. 2018. Soil bacterial community responses to altered precipitation and temperature regimes in an old field grassland are mediated by plants. FEMS Microbiol Ecol 94.

16. Simmons T, Styer AB, Pierroz G, Gonçalves AP, Pasricha R, Hazra AB, Bubner P, Coleman-Derr D. 2020. Drought Drives Spatial Variation in the Millet Root Microbiome. Front Plant Sci 11:599.

17. Baraniya D, Nannipieri P, Kublik S, Vestergaard G, Schloter M, Schöler A. 2018. The Impact of the Diurnal Cycle on the Microbial Transcriptome in the Rhizosphere of Barley. Microb Ecol 75:830–833.

18. Chaparro JM, Badri DV, Bakker MG, Sugiyama A, Manter DK, Vivanco JM. 2013. Root exudation of phytochemicals in Arabidopsis follows specific patterns that are developmentally programmed and correlate with soil microbial functions. PLoS One 8:e55731.

19. Zhalnina K, Louie KB, Hao Z, Mansoori N, da Rocha UN, Shi S, Cho H, Karaoz U, Loqué D, Bowen BP, Firestone MK, Northen TR, Brodie EL. 2018. Dynamic root exudate chemistry and microbial substrate preferences drive patterns in rhizosphere microbial community assembly. Nat Microbiol 3:470–480.

20. Wallace JG, Kremling KA, Kovar LL, Buckler ES. 2018. Quantitative Genetics of the Maize Leaf Microbiome. Phytobiomes Journal 2:208–224.

21. Badri DV, Chaparro JM, Zhang R, Shen Q, Vivanco JM. 2013. Application of natural blends of phytochemicals derived from the root exudates of Arabidopsis to the soil reveal that phenolic-related compounds predominantly modulate the soil microbiome. J Biol Chem 288:4502–4512.

22. Zhang N, Wang D, Liu Y, Li S, Shen Q, Zhang R. 2014. Effects of different plant

root exudates and their organic acid components on chemotaxis, biofilm formation and colonization by beneficial rhizosphere-associated bacterial strains. Plant Soil 374:689–700.

23. Huang AC, Jiang T, Liu Y-X, Bai Y-C, Reed J, Qu B, Goossens A, Nützmann H-W, Bai Y, Osbourn A. 2019. A specialized metabolic network selectively modulates Arabidopsis root microbiota. Science 364.

24. Cai T, Cai W, Zhang J, Zheng H, Tsou AM, Xiao L, Zhong Z, Zhu J. 2009. Host legume-exuded antimetabolites optimize the symbiotic rhizosphere. Mol Microbiol 73:507–517.

25. Bressan M, Roncato M-A, Bellvert F, Comte G, Haichar FZ, Achouak W, Berge O. 2009. Exogenous glucosinolate produced by Arabidopsis thaliana has an impact on microbes in the rhizosphere and plant roots. ISME J 3:1243–1257.

26. Iven T, König S, Singh S, Braus-Stromeyer SA, Bischoff M, Tietze LF, Braus GH, Lipka V, Feussner I, Dröge-Laser W. 2012. Transcriptional activation and production of tryptophan-derived secondary metabolites in arabidopsis roots contributes to the defense against the fungal vascular pathogen Verticillium longisporum. Mol Plant 5:1389–1402.

27. Wang Y, Bouwmeester K, van de Mortel JE, Shan W, Govers F. 2013. A novel Arabidopsis-oomycete pathosystem: differential interactions with Phytophthora capsici reveal a role for camalexin, indole glucosinolates and salicylic acid in defence. Plant Cell Environ 36:1192–1203.

757 28. Wang Z, Zhang J, Wu F, Zhou X. 2018. Changes in rhizosphere microbial
758 communities in potted cucumber seedlings treated with syringic acid. PLoS One
759 13:e0200007.

760 29. Hu L, Robert CAM, Cadot S, Zhang X, Ye M, Li B, Manzo D, Chervet N, Steinger T,
761 van der Heijden MGA, Schlaeppi K, Erb M. 2018. Root exudate metabolites drive
762 plant-soil feedbacks on growth and defense by shaping the rhizosphere microbiota.
763 Nat Commun 9:2738.

764 30. Xu L, Coleman-Derr D. 2019. Causes and consequences of a conserved bacterial
765 root microbiome response to drought stress. Curr Opin Microbiol 49:1–6.

766 31. Caddell DF, Deng S, Coleman-Derr D. 2019. Role of the Plant Root Microbiome in
767 Abiotic Stress Tolerance, p. 273–311. *In* Verma, SK, White, Jr, Francis, J (eds.),
768 Seed Endophytes: Biology and Biotechnology. Springer International Publishing,
769 Cham.

770 32. Bostock RM, Pye MF, Roubtsova TV. 2014. Predisposition in plant disease:
771 exploiting the nexus in abiotic and biotic stress perception and response. Annu Rev
772 Phytopathol 52:517–549.

773 33. Yasuda M, Ishikawa A, Jikumaru Y, Seki M, Umezawa T, Asami T, Maruyama-
774 Nakashita A, Kudo T, Shinozaki K, Yoshida S, Nakashita H. 2008. Antagonistic
775 interaction between systemic acquired resistance and the abscisic acid-mediated
776 abiotic stress response in Arabidopsis. Plant Cell 20:1678–1692.

777 34. Varoquaux N, Cole B, Gao C, Pierroz G, Baker CR, Patel D, Madera M, Jeffers T,

778 Hollingsworth J, Sievert J, Yoshinaga Y, Owiti JA, Singan VR, DeGraaf S, Xu L,
779 Blow MJ, Harrison MJ, Visel A, Jansson C, Niyogi KK, Hutmacher R, Coleman-Derr
780 D, O'Malley RC, Taylor JW, Dahlberg J, Vogel JP, Lemaux PG, Purdom E. 2019.
781 Transcriptomic analysis of field-droughted sorghum from seedling to maturity
782 reveals biotic and metabolic responses. Proc Natl Acad Sci U S A.

783 35. Sheflin AM, Chiniquy D, Yuan C, Goren E, Kumar I, Braud M, Brutnell T, Eveland
784 AL, Tringe S, Liu P, Kresovich S, Marsh EL, Schachtman DP, Prenni JE. 2019.
785 Metabolomics of sorghum roots during nitrogen stress reveals compromised
786 metabolic capacity for salicylic acid biosynthesis. Plant Direct 3:e00122.

787 36. Castrillo G, Teixeira PJPL, Paredes SH, Law TF, de Lorenzo L, Feltcher ME, Finkel
788 OM, Breakfield NW, Mieczkowski P, Jones CD, Paz-Ares J, Dangl JL. 2017. Root
789 microbiota drive direct integration of phosphate stress and immunity. Nature
790 543:513–518.

791 37. Hein JW, Wolfe GV, Blee KA. 2008. Comparison of rhizosphere bacterial
792 communities in Arabidopsis thaliana mutants for systemic acquired resistance.
793 Microb Ecol 55:333–343.

794 38. Carvalhais LC, Dennis PG, Badri DV, Kidd BN, Vivanco JM, Schenk PM. 2015.
795 Linking Jasmonic Acid Signaling, Root Exudates, and Rhizosphere Microbiomes.
796 Mol Plant Microbe Interact 28:1049–1058.

797 39. Liu H, Carvalhais LC, Schenk PM, Dennis PG. 2017. Effects of jasmonic acid
798 signalling on the wheat microbiome differ between body sites. Sci Rep 7:41766.

799 40. Lebeis SL, Paredes SH, Lundberg DS, Breakfield N, Gehring J, McDonald M,
800 Malfatti S, Glavina del Rio T, Jones CD, Tringe SG, Dangl JL. 2015. PLANT
801 MICROBIOME. Salicylic acid modulates colonization of the root microbiome by
802 specific bacterial taxa. Science 349:860–864.

803 41. Návarová H, Bernsdorff F, Döring A-C, Zeier J. 2012. Pipecolic acid, an
804 endogenous mediator of defense amplification and priming, is a critical regulator of
805 inducible plant immunity. Plant Cell 24:5123–5141.

806 42. Bernsdorff F, Döring A-C, Gruner K, Schuck S, Bräutigam A, Zeier J. 2016.
807 Pipecolic Acid Orchestrates Plant Systemic Acquired Resistance and Defense
808 Priming via Salicylic Acid-Dependent and -Independent Pathways. Plant Cell
809 28:102–129.

810 43. Bowen BP, Northen TR. 2010. Dealing with the unknown: metabolomics and
811 metabolite atlases. J Am Soc Mass Spectrom 21:1471–1476.

812 44. Cámara B, Bielecki P, Kaminski F, dos Santos VM, Plumeier I, Nikodem P, Pieper
813 DH. 2007. A gene cluster involved in degradation of substituted salicylates via ortho
814 cleavage in Pseudomonas sp. strain MT1 encodes enzymes specifically adapted for
815 transformation of 4-methylcatechol and 3-methylmuconate. J Bacteriol 189:1664–
816 1674.

817 45. Zhang K, Halitschke R, Yin C, Liu C-J, Gan S-S. 2013. Salicylic acid 3-hydroxylase
818 regulates Arabidopsis leaf longevity by mediating salicylic acid catabolism. Proc
819 Natl Acad Sci U S A 110:14807–14812.

820 46. Philip-Hollingsworth$ S, Hollingsworth RI, Dazzo ST FB. 1991. N-Acetylglutamic
821 Acid: An Extracellular nod Signal of Rhizobium trifolii ANUS43 That Induces Root
822 Hair Branching and Nodule-like Primordia in White Clover Roots. Plan Perspect
823 16854:16858.

824 47. Caspersen S, Sundin P, Munro M, Aðalsteinsson S, Hooker JE, Jensén P. 1999.
825 Interactive effects of lettuce (Lactuca sativa L.), irradiance, and ferulic acid in
826 axenic, hydroponic culture. Plant Soil 210:115–126.

827 48. Sakamoto A, Murata N. 2000. Genetic engineering of glycinebetaine synthesis in
828 plants: current status and implications for enhancement of stress tolerance. J Exp
829 Bot 51:81–88.

830 49. Moulin M, Deleu C, Larher F, Bouchereau A. 2006. The lysine-ketoglutarate
831 reductase-saccharopine dehydrogenase is involved in the osmo-induced synthesis
832 of pipecolic acid in rapeseed leaf tissues. Plant Physiol Biochem 44:474–482.

833 50. Goas G, Goas M, Larher F. 1976. Formation de l'acide pipécolique chez Triglochin
834 maritima. Can J Bot 54:1221–1227.

835 51. Bown AW, Shelp BJ. 2016. Plant GABA: Not Just a Metabolite. Trends Plant Sci
836 21:811–813.

837 52. Nourimand M, Todd CD. 2017. Allantoin contributes to the stress response in
838 cadmium-treated Arabidopsis roots. Plant Physiol Biochem 119:103–109.

839 53. Irani S, Todd CD. 2018. Exogenous allantoin increases Arabidopsis seedlings
840 tolerance to NaCl stress and regulates expression of oxidative stress response

841 genes. J Plant Physiol 221:43–50.

842 54. Khan N, Bano A, Babar MA. 2019. Metabolic and physiological changes induced by
843 plant growth regulators and plant growth promoting rhizobacteria and their impact
844 on drought tolerance in Cicer arietinum L. PLoS One 14:e0213040.

845 55. Oney-Birol S. 2019. Exogenous L-Carnitine Promotes Plant Growth and Cell
846 Division by Mitigating Genotoxic Damage of Salt Stress. Sci Rep 9:17229.

847 56. Ranieri A, Bernardi R, Lanese P, Soldatini GF. 1989. Changes in free amino acid
848 content and protein pattern of maize seedlings under water stress. Environ Exp Bot
849 29:351–357.

850 57. Rai VK. 2002. Role of amino acids in plant responses to stresses. Biol Plant.

851 58. Fang Y, Xiong L. 2015. General mechanisms of drought response and their
852 application in drought resistance improvement in plants. Cell Mol Life Sci 72:673–
853 689.

854 59. Gargallo-Garriga A, Preece C, Sardans J, Oravec M, Urban O, Peñuelas J. 2018.
855 Root exudate metabolomes change under drought and show limited capacity for
856 recovery. Sci Rep 8:12696.

857 60. Fàbregas N, Fernie AR. 2019. The metabolic response to drought. J Exp Bot
858 70:1077–1085.

859 61. Conn VM, Walker AR, Franco CMM. 2008. Endophytic actinobacteria induce
860 defense pathways in Arabidopsis thaliana. Mol Plant Microbe Interact 21:208–218.

861 62. Korenblum E, Dong Y, Szymanski J, Panda S, Jozwiak A, Massalha H, Meir S,
862 Rogachev I, Aharoni A. 2020. Rhizosphere microbiome mediates systemic root
863 metabolite exudation by root-to-root signaling. Proc Natl Acad Sci U S A 117:3874–
864 3883.

865 63. Wang C, Liu R, Lim G-H, de Lorenzo L, Yu K, Zhang K, Hunt AG, Kachroo A,
866 Kachroo P. 2018. Pipecolic acid confers systemic immunity by regulating free
867 radicals. Sci Adv 4:eaar4509.

868 64. Tsuji W, Inanaga S, Araki H, Morita S, An P, Sonobe K. 2005. Development and
869 Distribution of Root System in Two GrainSorghum Cultivars Originated from Sudan
870 under Drought Stress. Plant Prod Sci 8:553–562.

871 65. Sebastian J, Yee M-C, Goudinho Viana W, Rellán-Álvarez R, Feldman M, Priest
872 HD, Trontin C, Lee T, Jiang H, Baxter I, Mockler TC, Hochholdinger F, Brutnell TP,
873 Dinneny JR. 2016. Grasses suppress shoot-borne roots to conserve water during
874 drought. Proc Natl Acad Sci U S A 113:8861–8866.

875 66. Wang Y, Schuck S, Wu J, Yang P, Döring A-C, Zeier J, Tsuda K. 2018. A MPK3/6-
876 WRKY33-ALD1-Pipecolic Acid Regulatory Loop Contributes to Systemic Acquired
877 Resistance. Plant Cell 30:2480–2494.

878 67. Hartmann M, Zeier J. 2019. N-hydroxypipecolic acid and salicylic acid: a metabolic
879 duo for systemic acquired resistance. Curr Opin Plant Biol 50:44–57.

880 68. Hartmann M, Zeier T, Bernsdorff F, Reichel-Deland V, Kim D, Hohmann M,
881 Scholten N, Schuck S, Bräutigam A, Hölzel T, Ganter C, Zeier J. 2018. Flavin

882 Monooxygenase-Generated N-Hydroxypipecolic Acid Is a Critical Element of Plant
883 Systemic Immunity. Cell 173:456–469.e16.

884 69. Cao H, Bowling SA, Gordon AS, Dong X. 1994. Characterization of an Arabidopsis
885 Mutant That Is Nonresponsive to Inducers of Systemic Acquired Resistance. Plant
886 Cell 6:1583–1592.

887 70. Jung HW, Tschaplinski TJ, Wang L, Glazebrook J, Greenberg JT. 2009. Priming in
888 systemic plant immunity. Science 324:89–91.

889 71. Wang C, El-Shetehy M, Shine MB, Yu K, Navarre D, Wendehenne D, Kachroo A,
890 Kachroo P. 2014. Free radicals mediate systemic acquired resistance. Cell Rep
891 7:348–355.

892 72. Henry A, Doucette W, Norton J, Bugbee B. 2007. Changes in crested wheatgrass
893 root exudation caused by flood, drought, and nutrient stress. J Environ Qual
894 36:904–912.

895 73. Preece C, Farré-Armengol G, Llusià J, Peñuelas J. 2018. Thirsty tree roots exude
896 more carbon. Tree Physiol 38:690–695.

897 74. You J, Zhang Y, Liu A, Li D, Wang X, Dossa K, Zhou R, Yu J, Zhang Y, Wang L,
898 Zhang X. 2019. Transcriptomic and metabolomic profiling of drought-tolerant and
899 susceptible sesame genotypes in response to drought stress. BMC Plant Biol
900 19:267.

901 75. Holmes EC, Chen Y-C, Sattely E, Mudgett MB. 2019. Conservation of N-hydroxy-
902 pipecolic acid-mediated systemic acquired resistance in crop plants. bioRxiv.

903 76. He Q, Zhao S, Ma Q, Zhang Y, Huang L, Li G, Hao L. 2014. Endogenous Salicylic
904 Acid Levels and Signaling Positively Regulate Arabidopsis Response to
905 Polyethylene Glycol-Simulated Drought Stress. J Plant Growth Regul 33:871–880.

906 77. La VH, Lee B-R, Islam MT, Park S-H, Jung H-I, Bae D-W, Kim T-H. 2019.
907 Characterization of salicylic acid-mediated modulation of the drought stress
908 responses: Reactive oxygen species, proline, and redox state in Brassica napus.
909 Environ Exp Bot 157:1–10.

910 78. Ding Y, Dommel M, Mou Z. 2016. Abscisic acid promotes proteasome-mediated
911 degradation of the transcription coactivator NPR 1 in Arabidopsis thaliana. Plant J
912 86:20–34.

913 79. Schnake A, Hartmann M, Schreiber S, Malik J, Brahmann L, Yildiz I, von Dahlen J,
914 Rose LE, Schaffrath U, Zeier J. 2020. Inducible biosynthesis and immune function
915 of the systemic acquired resistance inducer N-hydroxypipecolic acid in
916 monocotyledonous and dicotyledonous plants. J Exp Bot.

917 80. Gouesbet G, Blanco C, Hamelin J, Bernard T. 1992. Osmotic adjustment in
918 Brevibacterium ammoniagenes: pipecolic acid accumulation at elevated
919 osmolalities. J Gen Microbiol 138:959–965.

920 81. Gouesbet G, Jebbar M, Talibart R, Bernard T, Blanco C. 1994. Pipecolic acid is an
921 osmoprotectant for Escherichia coli taken up by the general osmoporters ProU and
922 ProP. Microbiology 140 (Pt 9):2415–2422.

923 82. Gouffi K, Bernard T, Blanco C. 2000. Osmoprotection by pipecolic acid in

924 Sinorhizobium meliloti: specific effects of D and L isomers. Appl Environ Microbiol
925 66:2358–2364.

926 83. Neshich IAP, Kiyota E, Arruda P. 2013. Genome-wide analysis of lysine catabolism
927 in bacteria reveals new connections with osmotic stress resistance. ISME J 7:2400–
928 2410.

929 84. Gao C, Montoya L, Xu L, Madera M, Hollingsworth J, Purdom E, Singan V, Vogel J,
930 Hutmacher RB, Dahlberg JA, Coleman-Derr D, Lemaux PG, Taylor JW. 2020.
931 Fungal community assembly in drought-stressed sorghum shows stochasticity,
932 selection, and universal ecological dynamics. Nat Commun 11:34.

933 85. Simmons T, Caddell DF, Deng S, Coleman-Derr D. 2018. Exploring the Root
934 Microbiome: Extracting Bacterial Community Data from the Soil, Rhizosphere, and
935 Root Endosphere. J Vis Exp.

936 86. Bolyen E, Rideout JR, Dillon MR, Bokulich NA, Abnet CC, Al-Ghalith GA, Alexander
937 H, Alm EJ, Arumugam M, Asnicar F, Bai Y, Bisanz JE, Bittinger K, Brejnrod A,
938 Brislawn CJ, Brown CT, Callahan BJ, Caraballo-Rodríguez AM, Chase J, Cope EK,
939 Da Silva R, Diener C, Dorrestein PC, Douglas GM, Durall DM, Duvallet C,
940 Edwardson CF, Ernst M, Estaki M, Fouquier J, Gauglitz JM, Gibbons SM, Gibson
941 DL, Gonzalez A, Gorlick K, Guo J, Hillmann B, Holmes S, Holste H, Huttenhower C,
942 Huttley GA, Janssen S, Jarmusch AK, Jiang L, Kaehler BD, Kang KB, Keefe CR,
943 Keim P, Kelley ST, Knights D, Koester I, Kosciolek T, Kreps J, Langille MGI, Lee J,
944 Ley R, Liu Y-X, Loftfield E, Lozupone C, Maher M, Marotz C, Martin BD, McDonald
945 D, McIver LJ, Melnik AV, Metcalf JL, Morgan SC, Morton JT, Naimey AT, Navas-

946 Molina JA, Nothias LF, Orchanian SB, Pearson T, Peoples SL, Petras D, Preuss
947 ML, Pruesse E, Rasmussen LB, Rivers A, Robeson MS 2nd, Rosenthal P, Segata
948 N, Shaffer M, Shiffer A, Sinha R, Song SJ, Spear JR, Swafford AD, Thompson LR,
949 Torres PJ, Trinh P, Tripathi A, Turnbaugh PJ, Ul-Hasan S, van der Hooft JJJ,
950 Vargas F, Vázquez-Baeza Y, Vogtmann E, von Hippel M, Walters W, Wan Y, Wang
951 M, Warren J, Weber KC, Williamson CHD, Willis AD, Xu ZZ, Zaneveld JR, Zhang Y,
952 Zhu Q, Knight R, Caporaso JG. 2019. Reproducible, interactive, scalable and
953 extensible microbiome data science using QIIME 2. Nat Biotechnol 37:852–857.

954 87. Callahan BJ, McMurdie PJ, Rosen MJ, Han AW, Johnson AJA, Holmes SP. 2016.
955 DADA2: High-resolution sample inference from Illumina amplicon data. Nat
956 Methods 13:581–583.

957 88. Development Core Team RR. 2011. R: A language and environment for statistical
958 computing.

959 89. McMurdie PJ, Holmes S. 2013. phyloseq: an R package for reproducible interactive
960 analysis and graphics of microbiome census data. PLoS One 8:e61217.

961 90. Dixon P. 2003. VEGAN, a package of R functions for community ecology. J Veg Sci
962 14:927–930.

963 91. Yao Y, Sun T, Wang T, Ruebel O, Northen T, Bowen BP. 2015. Analysis of
964 Metabolomics Datasets with High-Performance Computing and Metabolite Atlases.
965 Metabolites 5:431–442.

966 92. Smith CA, O'Maille G, Want EJ, Qin C, Trauger SA, Brandon TR, Custodio DE,

967 Abagyan R, Siuzdak G. 2005. METLIN: a metabolite mass spectral database. Ther
968 Drug Monit 27:747–751.

969 93. Oliveros JC. 2016. Venny. An interactive tool for comparing lists with Venn's
970 diagrams. 2007--2015.

971 94. Chong J, Soufan O, Li C, Caraus I, Li S, Bourque G, Wishart DS, Xia J. 2018.
972 MetaboAnalyst 4.0: towards more transparent and integrative metabolomics
973 analysis. Nucleic Acids Res 46:W486–W494.

974 95. Chong J, Wishart DS, Xia J. 2019. Using MetaboAnalyst 4.0 for Comprehensive
975 and Integrative Metabolomics Data Analysis. Curr Protoc Bioinformatics 68:e86.

976 96. Mishina TE, Zeier J. 2006. The Arabidopsis flavin-dependent monooxygenase
977 FMO1 is an essential component of biologically induced systemic acquired
978 resistance. Plant Physiol 141:1666–1675.

979 97. Cao H, Glazebrook J, Clarke JD, Volko S, Dong X. 1997. The Arabidopsis NPR1
980 gene that controls systemic acquired resistance encodes a novel protein containing
981 ankyrin repeats. Cell 88:57–63.

982 98. Torres MA, Dangl JL, Jones JDG. 2002. Arabidopsis gp91phox homologues
983 AtrbohD and AtrbohF are required for accumulation of reactive oxygen
984 intermediates in the plant defense response. Proc Natl Acad Sci U S A 99:517–522.

985 99. Lamesch P, Berardini TZ, Li D, Swarbreck D, Wilks C, Sasidharan R, Muller R,
986 Dreher K, Alexander DL, Garcia-Hernandez M, Karthikeyan AS, Lee CH, Nelson
987 WD, Ploetz L, Singh S, Wensel A, Huala E. 2012. The Arabidopsis Information

988 Resource (TAIR): improved gene annotation and new tools. Nucleic Acids Res
989 40:D1202–10.

990 100. Schneider CA, Rasband WS, Eliceiri KW. 2012. NIH Image to ImageJ: 25 years
991 of image analysis. Nat Methods 9:671–675.

Tables

Table 1. Detailed information on significantly changed metabolites between drought and watered roots

Proposed metabolite	Molecular formula	Measured *m/z*	ppm error	Measured RT peak (minutes)	RT error	MSMS quality score*	Ion mode	Log2 (FC)	p-value (root)	q-value (root)	Significant compartment(s)**
methionine	C5H11NO2S	148.044	1.748	10.6	0.1	1	negative	3.21	0.001	0.016	RZS
proline	C5H9NO2	116.071	2.444	11.1	0.1	1	positive	2.82	0.001	0.016	RZS
betaine	C5H12NO2+	118.087	2.456	7.8	0.2	1	positive	2.48	0.000	0.016	RZS
carnitine	C7H16NO3+	162.113	0.503	13.2	0.2	1	positive	2.43	0.012	0.038	RZS
N-trimethyllysine	C9H21N2O2+	189.160	0.178	16.8	0.1	1	positive	5.49	0.002	0.020	RZ
3-hydroxykynurenine	C10H12N2O4	225.087	0.497	11.2	0.1	0	positive	4.54	0.012	0.038	RZ
lysine	C6H14N2O2	147.113	0.569	17.0	0.1	1	positive	4.24	0.001	0.016	RZ
taurine	C2H7NO3S	126.022	1.176	12.3	0.0	0	positive	3.94	0.012	0.038	RZ
arginine	C6H14N4O2	175.119	0.691	17.0	0.1	1	positive	3.81	0.002	0.018	RZ
pipecolic acid	C6H11NO2	130.086	0.888	11.0	0.0	1	positive	3.39	0.001	0.016	RZ
allothreonine// homoserine// threonine	C4H9NO3	120.066	1.912	13.7	0.1	0	positive	3.25	0.003	0.021	RZ
valine	C5H11NO2	116.072	1.809	11.2	0.0	1	negative	3.15	0.003	0.020	RZ
1-aminocyclopropane-1-carboxylic acid	C4H7NO2	102.055	3.955	13.7	0.6	1	positive	3.14	0.003	0.020	RZ
2-amino-2-methylpropanoic acid	C4H9NO2	104.071	4.409	12.5	0.0	1	positive	2.98	0.004	0.025	RZ
asparagine	C4H8N2O3	133.061	0.814	14.5	0.1	1	positive	2.91	0.006	0.027	RZ
cis-4-hydroxy-proline//trans-4-hydroxyproline	C5H9NO3	130.051	0.823	13.4	0.3	0	negative	2.90	0.004	0.022	RZ
guanidinoacetic acid	C3H7N3O2	118.061	2.161	14.0	0.1	0	positive	2.43	0.003	0.020	RZ
deoxycarnitine	C7H16NO2+	146.118	0.662	13.3	0.2	1	positive	2.39	0.024	0.061	RZ
serotonin	C10H12N2O	177.102	0.870	8.7	0.1	0	positive	3.47	0.042	0.087	RO
histidinol	C6H11N3O	142.098	0.107	12.9	0.2	0	positive	2.95	0.014	0.044	RO
trans-4-hydroxyproline	C5H9NO3	132.066	0.768	13.4	0.1	0	positive	2.83	0.004	0.022	RO
o-acetyl-serine	C5H9NO4	148.060	0.072	11.4	0.1	-1	positive	2.83	0.016	0.045	RO
4-methoxyphenylacetic acid	C9H10O3	184.097	0.912	1.1	0.0	0	positive	2.79	0.005	0.026	RO
riboflavin	C17H20N4O6	377.146	1.147	4.6	0.0	0	positive	2.67	0.004	0.025	RO
hippuric acid	C9H9NO3	180.066	0.924	4.6	0.3	0	positive	2.41	0.009	0.034	RO
acetylcholine	C7H16NO2+	146.118	0.496	2.1	0.1	1	positive	2.38	0.010	0.036	RO
pyridoxamine	C8H12N2O2	169.097	0.267	10.2	0.0	0	positive	2.12	0.001	0.016	RO
abscisic acid	C15H20O4	247.133	1.332	1.1	0.0	0	positive	2.05	0.006	0.026	RO
2,3-dihydroxybenzoic acid// 2,5-dihydroxybenzoic acid// 3,4-dihydroxybenzoic acid	C7H6O4	153.020	1.467	4.0	0.1	0	negative	-2.11	0.000	0.012	RO
xylitol	C5H12O5	175.058	4.087	5.1	0.0	0	positive	-3.16	0.001	0.016	RO
4-methylcatechol	C7H8O2	123.045	1.158	4.3	0.4	0	negative	-3.73	0.001	0.016	RO

*MSMS quality scores: 1 (MSMS matches ref. std.); 0.5 (possible match); 0 (no MSMS collected or no appropriate ref available); -1 (MSMS poor match to ref. std.)

**Compartment(s) with significant Log2 (fold change): Root, rhizosphere, and soil (RZS); root and rhizosphere (RZ); root only (RO)

997 Table 2. Detailed information on significantly changed metabolites 24 hours after

998 rewatering

Proposed metabolite	Molecular formula	Measured *m/z*	ppm error	Measured RT peak (minutes)	RT error	MSMS quality score*	Ion mode	Log2 (FC)	p-value (root)	q-value (root)	Significant compartment
4-imidazoleacetic acid	C5H6N2O2	127.050	0.936	13.9	0.2	1	positive	-2.44	0.049	0.296	rhizosphere
1-aminocyclopropane-1-carboxylic acid	C4H7NO2	102.055	3.955	13.7	0.6	1	positive	-2.44	0.047	0.296	rhizosphere
pipecolic acid	C6H11NO2	130.086	0.888	11.0	0.0	1	positive	-2.45	0.048	0.296	rhizosphere
carnitine	C7H16NO3+	162.113	0.503	13.2	0.2	1	positive	-2.49	0.017	0.231	rhizosphere
melatonin	C13H16N2O2	233.128	1.296	1.2	0.0	0	positive	-2.89	0.011	0.213	rhizosphere
3-hydroxyanthranilic acid	C7H7NO3	152.036	1.229	1.8	0.1	0	negative	-3.11	0.003	0.135	rhizosphere
syringic acid	C9H10O5	197.046	0.404	1.6	0.1	1	negative	-3.42	0.040	0.296	rhizosphere
cytidine 2',3'-cyclic mono-phosphoric acid	C9H12N3O7P	306.049	1.863	14.0	0.2	0	positive	-3.44	0.047	0.296	rhizosphere
abscisic acid	C15H20O4	247.133	1.332	1.1	0.0	0	positive	-3.56	0.002	0.135	rhizosphere
galactitol//mannitol	C6H14O6	181.072	1.680	9.7	0.1	1	negative	-3.58	0.026	0.263	rhizosphere
4-methylcatechol	C7H8O2	123.045	1.158	4.3	0.4	0	negative	-4.45	0.005	0.169	rhizosphere
2,3-dihydroxybenzoic acid// 2,5-dihydroxybenzoic acid// 3,4-dihydroxybenzoic acid	C7H6O4	153.020	1.467	4.0	0.1	0	negative	-4.45	0.040	0.296	rhizosphere
erythritol	C4H10O4	121.051	0.626	3.2	0.0	1	negative	-5.04	0.024	0.252	rhizosphere
arabitol	C5H12O5	151.061	1.358	5.6	0.2	1	negative	-5.29	0.003	0.135	rhizosphere
sn-glycero-3-phosphocholine	C8H21NO6P+	258.110	0.111	14.8	0.2	1	positive	-5.66	0.017	0.231	rhizosphere
guanosine 3',5'-cyclic monophosphoric acid	C10H12N5O7P	346.055	0.947	13.9	0.2	0	positive	-5.73	0.000	0.019	rhizosphere
ferulic acid	C10H10O4	193.051	0.614	1.3	0.1	1	negative	-5.75	0.008	0.181	rhizosphere
lactose//trehalose	C12H22O11	401.131	1.143	14.4	0.1	1	negative	-3.07	0.002	0.340	soil

*MSMS quality scores: 1 (MSMS matches ref. std.); 0.5 (possible match); 0 (no MSMS collected or no appropriate ref available); -1 (MSMS poor match to ref. std.)

999

1000

Figure captions

Figure 1. Sorghum root-associated microbiome responds to drought and rewatering. A Representative image of sorghum plants following eight weeks of a preflowering drought (TP8). **B** Phylum level relative abundances of sorghum root, rhizosphere, and soil microbiomes at TP8 and 24 hours after rewatering (24h DW) in well-watered (W) or drought (D) plots. **C** Alpha diversity (Shannon) of sorghum root, rhizosphere, and soil. **D** Beta diversity (PCoA) of sorghum root, rhizosphere, and soil microbiomes at TP8 and 24 hours after rewatering in well-watered control or drought plots. **E-J** Relative abundances of individual lineages that displayed a significant difference in abundance between watering treatments (ANOVA, Tukey-HSD, $P<0.05$).

Figure 2. Metabolic profiles during drought differ by compartment. A Heatmap of relative peak heights of all observed metabolites (n=168) across root, rhizosphere (rhizo), and soil compartments and watered (W) and drought (D) treatments. **B** Principal component analysis (PCA) plot of root, rhizosphere, and soil metabolites. **C** Proportional Venn diagram of drought enriched metabolites in root, rhizosphere, or soil (D/W Log_2 fold change >2, t-test $p<0.05$). **D-E** Heatmap of the subset of metabolites that were enriched or depleted in roots during drought, with the predicted identity of metabolites listed beside each row.

Figure 3. Rewatering depletes rhizosphere metabolites following a prolonged drought. A Heatmap of relative peak heights of all observed metabolites (n=168)

across three compartments (root, rhizosphere (rhizo), and soil), three treatments (watered (W), drought (D), drought rewatered (DW), and two time points (time point 8 (TP8) and 24 hours later (24h)). **B-C** Heatmap of the subset of metabolites that were depleted after rewatering (DW/D Log_2 fold change < -2, t-test $p<0.05$), with the predicted identity of metabolites listed beside each row. Note, all significant depletions were observed in the rhizosphere, except trehalose, which occurred in soil. **D** Principal component analysis (PCA) plot of root, rhizosphere, and soil metabolites.

Figure 4. Pipecolic acid abundance pattern mirrors drought markers. A The top 10 metabolites correlated with the drought marker betaine across all sample types, treatments, and time points. **B-D** Log_{10} peak heights of individual metabolites. Each point represents an individual sample of root (green), rhizosphere (blue), or soil (yellow). Dashed lines represent the limit of detection for individual metabolites, based on the average log_{10} peak heights of the sample blanks for root (red) or rhizosphere and soil (blue). **E** Heatmap of relative abundance of all metabolites and bacteria ASVs (grouped at the class level), clustered within the root, across treatments (watered (W), drought (D), drought rewatered (DW), and time points (time point 8 (TP8) and 24 hours later (24h)). **F** Zoom-in of Actinobacteria and closely clustering root metabolites, as highlighted in pink in figure 4e. Actinobacteria and the metabolites that are closely correlated with betaine (as in figure 4a) are in bold.

Figure 5. Pipecolic acid reduces root growth. A Root lengths of sterilized sorghum seedlings after 7 days of growth in water containing 0, 0.1, or 1 mM pipecolic acid (Pip).

Different letters indicate a significant difference in root length (ANOVA, Tukey-HSD, $p<0.05$). This experiment was performed twice with similar results. **B** Two representative seedlings from each treatment were photographed at the time of measurement. **C** Root lengths of sterilized Arabidopsis seedlings after 10 days of growth in ½ MS+ 1% sucrose agar media containing 0, 0.001, 0.01, 0.1, or 1 mM Pip. Different letters indicate a significant difference in root length (ANOVA, Tukey-HSD, $p<0.05$). Different colors represent plants from independent experiments (n=3). **D** One representative plate from 0 and 1 mM pipecolic acid treatments were photographed at the time of measurement.

Figure 6. Pipecolic acid root growth reduction is SAR-independent. A Root length of Arabidopsis Col-0 (WT) and Arabidopsis mutants grown on 1/2MS + 1% sucrose plates containing 0 or 1 mM Pip. Significance between treatments was evaluated by ANOVA with Tukey's HSD posthoc test ($p<0.05$). Different colors represent plants from independent experiments. **B** Simplified SAR pathway. Highlighted in red are the Arabidopsis mutants used to evaluate a potential interaction between SAR and Pip-mediated root growth suppression.